RSC Advances

PAPER

View Article Online
View Journal | View Issue

Cite this: *RSC Adv.*, 2022, **12**, 11913

Electrospun porous poly(3-hydroxybutyrate-*co*-4-hydroxybutyrate)/lecithin scaffold for bone tissue engineering†

Wei Liu,‡[a] Tiejun Jiao,‡[b] Yuran Su,[a] Ran Wei,[a] Zheng Wang,[a] Jiacheng Liu,[a] Na Fu*[b] and Lei Sui *[a]

Bone tissue engineering has emerged as a promising restorative strategy for bone reconstruction and bone defect repair. It is challenging to establish an appropriate scaffold with an excellent porous microstructure for bone defects and thereby promote bone repair. In this study, electrospinning as a simple and efficient technology was employed to fabricate a porous poly(3-hydroxybutyrate-*co*-4-hydroxybutyrate) (P34HB) scaffold coated with lecithin. The morphology, phase composition, and physical properties of the electrospun P34HB/lec scaffold were characterized. Meanwhile, cellular behaviors of bone marrow mesenchymal stem cells (BMSCs), including proliferation, adhesion, migration, osteogenic differentiation, and related gene expression, were also investigated. Finally, a rat subcutaneous implant model and a calvarial defect model were used to evaluated the biocompatibility and effect of these scaffolds on bone repair, respectively. The *in vitro* results demonstrated that these electrospun fibers were interwoven with each other to form the porous P34HB/lec scaffold and the addition of lecithin improved the hydrophilicity of the pure P34HB scaffold, enhanced the efficiency of cell migration, and decreased inflammatory response. Furthermore, the *in vivo* results showed that P34HB/lec scaffold had excellent biocompatibility, improved the vascularization, and promoted the bone regeneration. All these results indicated that nanofibers of P34HB scaffolds in combination with the lecithin could exert a synergistic effect on promoting osteogenesis and regeneration of bone defects; thus, the P34HB scaffold with lecithin showed great application potential for bone tissue engineering.

Received 2nd March 2022
Accepted 8th April 2022

DOI: 10.1039/d2ra01398c

rsc.li/rsc-advances

1. Introduction

As a promising restorative treatment for bone defects, tissue engineering has attracted extensive attention in basic and clinical research.[1] The biological structures used in tissue engineering should have the potential to allow cell growth and differentiation, in order to integrate with surrounding tissue.[2] In this regard, various engineered scaffolds have been developed and play a vital role in the formation of new regeneration bone tissue.[3] A desirable tissue scaffold should be designed to mimic the extracellular matrix (ECM) of the intended tissue and should also provide appropriate topography, three-dimensional space, and chemical environment for efficient cell adhesion, proliferation, and differentiation.[4] Besides the construction of engineering scaffolds, the selection of scaffold material is regarded as fundamental to tissue engineering.[5] The biomaterials of engineering scaffolds include natural materials extracted from biological bodies and synthetic macromolecule materials and the latter have gained considerable attention in tissue engineering applications recently due to their favorable controllability, good processability and flexible mechanical properties.[6–8]

Poly(3-hydroxybutyrate-*co*-4-hydroxybutyrate) copolymer (P34HB), as a fourth generation polymer of polyhydroxyalkanoate (PHA) family, has become a promising scaffold material.[5] Unlike other conventional petrochemical polymers, the biopolymer P34HB could be naturally produced through bacterial and archaeal fermentation.[9] P34HB has great biocompatibility, appropriate biodegradability, and minimal tissue toxicity, demonstrating its good application potential in biomedicine.[10,11] P34HB also shows adjustable mechanical properties as well as high plasticity, and thus could be processed into different shapes according to various clinical requirements.[12,13] P34HB copolymer with different fractions of 4-hydroxybutyric (4HB) exhibits the highly adjustable elasticity and strength.[14] The biodegradability of PHAs depends on different factors, such as the composition of biopolymer, its stereo regularity, crystallinity, molecular mass, and

[a]*Department of Prosthodontics, School & Hospital of Stomatology, Tianjin Medical University, Tianjin 30070, China. E-mail: suilei@tmu.edu.cn*

[b]*Department of Implant, School & Hospital of Stomatology, Tianjin Medical University, Tianjin 30070, China. E-mail: 303141816@qq.com*

† Electronic supplementary information (ESI) available. See https://doi.org/10.1039/d2ra01398c

‡ Wei Liu and Tiejun Jiao contributed equally to this work.

environmental conditions.[9] Unlike the poly(3-hydroxybutyric) (PHB) homopolymer of PHA family, the molecular weight of P34HB copolymer could be increased as the 4HB fraction increases.[15] However, P34HB copolymer has a higher biodegradation rate *in vitro* due to the fast degradation of its amorphous regions and PHB homopolymer remained nearly unchanged with high crystallinity.[16,17] Besides, the degradation products of P34HB are oligo-hydroxyalkanoates which showed positive effects on cell growth.[18] Compared with other biopolymer materials applied in tissue engineering such as poly(lactide-*co*-glycolide acid) (PLGA) and poly(lactic acid) (PLA), the biodegradation rate of P34HB is much slower, thus, P34HB is more suitable for applications requiring slower degradation, especially for the bone tissue engineering.[19,20] Furthermore, compared to PLGA and PCL, P34HB could also remain stable local pH value during degradation, showing better tolerance to cells and immune system.[9,21] Though the previous researches of P34HB have mainly focused on the repair of the cardiac, skin, and organ tissue, P34HB also possesses the application potential in bone tissue engineering.[22–24]

Although there are many strategies employed in the fabrication of tissue engineering scaffolds, electrospinning has become an attractive technology in recent years, which could not only process many different polymers but also be operated simply.[25] This technology could produce numerous nanofibers with diameters from tens of nanometers to micrometers, constructing different types of tissue engineering scaffolds.[26,27] Through the electrospinning technology, the nanofiber scaffolds fabricated from different polymers as the raw materials possess high microporosity and enlarged specific surface area, providing a hierarchical structure similar to nature ECM and bone environment.[5,27,28]

Based on these advantages of P34HB and electrospinning technology, some studies have investigated the application of P34HB nanofiber scaffolds in bone tissue engineering. Fu *et al.* compared electrospun P34HB nanofiber scaffold to P34HB deposited film.[2] These two types of P34HB could accommodate growth, proliferation, and differentiation of adipose-derived stem cells (ASCs). Moreover, electrospun P34HB fibers showed better cell behavior.[2,29] Additionally, some inorganic materials such as graphene, graphene oxide, and octacalcium phosphate, were introduced into P34HB to construct different electrospun scaffolds for bone tissue engineering.[30–32] However, in these previous studies, electrospun P34HB scaffolds showed poor hydrophilicity with large water contact angles. These properties might have negative effects on its ability of promoting bone repair[33] and thus, need to be improved.

In order to improve hydrophilicity of P34HB scaffold, mimicking the biological membrane might be a promising approach.[34] Soy lecithin, as a main component of biological membrane, is a natural amphiphilic blend of phospholipids with a charged phosphatidylcholine head and two hydrocarbon tails.[35] Due to its amphiphilic structure, soy lecithin can aligned itself to form a hydrophilic and cytocompatible surface.[36] Several studies have focused on the modification of bone scaffold with lecithin and the modified scaffold with improved hydrophilicity is promising for tissue engineering applications such as bone graft and vascular graft.[37–39] Hence, these studies about the modification on scaffold with soy lecithin provided an available approach for improving hydrophilicity of electrospun P34HB scaffold.

Therefore, the aim of this study was to fabricate a hydrophilic electrospun P34HB scaffold *via* self-assembly of soy lecithin on the scaffold surface which could enhance bone regeneration. In the present research, the P34HB nanofibrous scaffolds, lecithin-assembled or lecithin-free, were constructed. Morphology, elemental composition analysis, porosity, and hydrophilicity of the electrospun scaffolds were characterized and compared. Then we explored the cellular behaviors of bone marrow mesenchymal stem cells (BMSCs) seeded on each scaffold, including morphology, viability, adhesion, proliferation, and osteogenesis. Finally, an animal study on rat calvarial-defect model was employed to evaluate the effect of lecithin-assembled fibrous scaffolds. This study demonstrates the fabrication and modification of P34HB scaffold with soy lecithin and sheds some light on its positive effect of promoting osteogenesis on bone defects.

2. Materials and methods

2.1. Materials

P34HB (M_w: 2.95×10^5, 89% 3HB and 11% 4HB) was ordered from Blue PHA (Beijing, China). 1,1,1,2,2,2-hexafluoro-2-propanol (HFIP) and absolute alcohol were purchased from Sigma-Aldrich (Darmstadt, Germany). Soy lecithin was purchased from Yuanye company (Shanghai, China). Fetal bovine serum (FBS), α-minimum essential medium (α-MEM), trypsin, and penicillin/streptomycin (PS) were purchased from Gibco (New York, USA). CCK-8 kit, FITC-phalloidin, DAPI and alizarin red staining kit were purchased from Solarbio (Beijing, China). ALP activity kit was purchased from Jiancheng company (Nanjing, China). The RT-PCR kits were purchased from TRANS company (Beijing, China). Sprague-Dawley (SD) rats were supplied by Charles River company (Beijing, China). All the chemical reagents mentioned above were of analytical grade and were used as received without further purification.

2.2. Fabrication of P34HB/lecithin porous scaffolds *via* electrospinning technology

In this study, 0.8 g macromolecule compound P34HB (Bluepha, China) was dissolved in 10 mL HFIP (Merck, Germany) to obtain 8% (w/v) mixed polymer solution for electrospinning. After stirred overnight with a magnetic stirrer, the polymer solution was loaded into a standard syringe attached with a 21 G blunted stainless-steel needle. A high voltage of 15 kV was used and the mixed polymer solution was pumped to form a Taylor pendant drop which was then elongated as a fiber under electric field. A rotating collector (SS-2535, Ucalery) with a speed of 120 rpm was applied and the distance between the roller and needle tip was adjusted at 15 cm to collect the aligned fibers. Soy lecithin (Yuanye, China) solution at a concentration of 10 μg mL^{-1} (ref. 40) was prepared by dissolved in absolute alcohol (Sigma-Aldrich, China). The electrospun scaffolds collected on the

rotating collector were soaked in soy lecithin solution for 10 min. Finally, electrospun P34HB fiber scaffolds as well as the scaffolds with lecithin were dried overnight in vacuum to evaporate the residual organic solvent. Hence, in this paper, the pure P34HB scaffolds and electrospun P34HB fiber scaffolds with the lecithin are denoted as P34HB and P34HB/lec.

2.3. Characterization of P34HB/lecithin electrospun fiber scaffold

The micro-morphology of these scaffolds was observed by a scanning electron microscopy (SEM) (Quanta FEG, FEI). The scaffolds were treated by desiccation and spray-gold, and then examined by SEM with an accelerating voltage of 20 kV. To identify the successful load of soy lecithin, surface properties of these scaffolds were examined by attenuated total reflection Fourier transform infrared (ATR-FTIR) spectroscopy (Nicolet 6700, Thermo Scientific).

Static drop contact angles of deionized water droplets on the scaffold were determined by an optical contact angle goniometer (KSV Instruments, Monroe), equipped with a digital camera to capture the images. Results were analyzed with Image J.

Protein adsorption was assessed according to the published assay.[41] After ultraviolet disinfection, the scaffolds in these different groups were put into a 24-well culture plate. Then 1 mL sterile PBS containing 10% FBS was added into each well of culture plate and the scaffolds were cultured for 24 h. The absorbance of cultured solution was determined at 290 nm by a microplate reader (Epoch2, Biotek).

Hemocompatibility was evaluated according to the published assay.[41] Briefly, red blood cells were obtained from the whole blood of SD rat and washed with 0.9% normal saline (0.9% NaCl) by centrifugation. Then red blood cells were diluted with 0.9% normal saline to obtain 4% (v/v) cell suspension. 0.5 mL deionized water was added into 0.5 mL cell suspension as positive control, while 0.5 mL cell suspension diluted with 0.5 mL saline was used as negative control. Besides, scaffolds of different groups were soaked into the red blood cell suspensions for 3 h, respectively. After centrifugation with 1500 rpm for 10 min, the absorbance of supernatant was examined at 540 nm by a microplate reader (Epoch2, Biotek). Hemolysis of scaffolds was contrasted according to the absorbance of different groups.

2.4. *In vitro* study

2.4.1. Cell culture. Bone marrow mesenchymal stem cells (BMSCs) were extracted from healthy 2 week-old SD rats according to the previously published procedures.[42] The obtained cells were incubated in α-MEM (MEM, Gibco) supplemented with 10% fetal bovine serum (FBS, Gibco) and 1% penicillin-streptomycin (PS, Gibco) under a culture condition of 37 °C and 5% CO_2. The culture medium of BMSCs was changed every 2 days and the cells were subcultured every 6 days. The third passage of rat BMSCs were used for cell experiments in this study.

2.4.2. Biocompatibility assay. Cell proliferation on the scaffolds was assessed by the cell counting kit-8 (CCK-8, Solarbio). BMSCs were seeded on the surface of scaffolds with a cell density of 1×10^4 cells per mL and cultured for 3, 5, or 7 days. The cells were rinsed twice with PBS and then 300 μL fresh medium containing 10% CCK-8 solution was added into each well. After incubation for 2 h at 37 °C, 100 μL of the supernatant per well was transferred into a 96-well plate and a microplate reader (Epoch2, Biotek) was applied to measure the absorbance of solution at 450 nm. The proliferation of cells on different scaffolds was assessed according to the absorbance of different groups.

Cell morphology on the scaffold surface was observed by laser scanning confocal microscopy (LSCM). Cells were seeded on the scaffolds (P34HB and P34HB/lec) at a cell density of 1×10^4 cells per mL. After 24 h, cells were rinsed twice with PBS and then fixed with 4% paraformaldehyde (PFA) at room temperature for 20 min. 0.5% Triton X-100 was used to permeabilize the cells for 5 min. The specimens were finally stained with FITC-phalloidin and DAPI in the dark according to the manufacturer's instructions. All these images were captured by a fluorescence microscope (LSM900, Zeiss).

The scratch test was conducted to assess the effect of soy lecithin on cell migration *in vitro*. Blank horizontal lines were drawn on the back of 6-well plate and BMSCs were seeded on the scaffolds in this plate with a cell density of 10×10^4 cells per mL. When the cells reached 90% confluence, a sterile pipet tip was used to create a scratch perpendicular to the blank horizontal lines in the middle of each well. Then the media containing different electrospun scaffolds of P34HB and P34HB/lec groups were added into the corresponding wells. Images of the migration assay were captured at 0 h, 8 h, 24 h, and 48 h by an optical microscope (Primovert, Zeiss).

2.4.3. Osteogenic differentiation. An osteogenic induction medium supplemented with 10 mM β-glycerol phosphate, 0.2 mM ascorbic acid, and 100 nM dexamethasone was used for the following osteogenic-related assays. The osteogenic medium was refreshed every 2 days.

Alkaline phosphatase (ALP) staining and the quantitative assay of ALP secretion were used to assess the osteogenic activities of BMSCs in four groups. BMSCs were seeded on the scaffolds at a cell density of 10×10^4 cells per mL. After culturing for 7 and 14 days, BCIP/NBT kit was applied for ALP staining and ALP activity kit (P0321, Jiancheng) was also used for quantitative analysis of ALP activity according to their manufacturer's instructions, respectively.

Extracellular matrix (ECM) mineralization was detected by alizarin red staining. BMSCs were seeded on the scaffolds (P34HB and P34HB/lec) at a cell density of 10×10^4 cells per mL. At 14 days, the samples were stained with alizarin red staining (Alizarin Red S, Solarbio) and then examined under a stereomicroscope (SZ810, Cnoptec). As for quantitative analysis, 10% cetylpyridinium chloride was added into each well to dissolve the alizarin red stain and the absorbance of solutions were measured at 542 nm by a microplate reader (Epoch2, Biotek). The experiments were repeated three times.

Real time-quantitative polymerase chain reaction (RT-PCR) was used to quantify the osteogenic gene expression of BMSCs on scaffolds. Cells were seeded on the scaffolds at a cell density

of 10×10^4 cells per mL and incubated for 7 or 14 days. BMSCs were harvested from the scaffolds by trypsin digestion and the cell suspension was centrifugated at 1500 rpm for 10 min. The total RNA was extracted by the Trizol method and the concentrations of RNA were determined by a spectrophotometry (Nanodrop, Thermo Scientific). Then RNA was reverse-transcribed to complementary DNA (cDNA) and then the quantification of cDNA was performed according to the standard protocol (EasyScript, Trans). Gene expression of *ALP* and *Col1a1* were detected as markers for early and late osteogenesis. The relative expression levels of these target genes were normalized based on the expression levels of the reference gene *GAPDH*. These experiments were conducted in triplicate. The primer sequences are listed in Table 1.

2.5. *In vivo* study

2.5.1. Animals. The animal use protocol has been reviewed and approved by the animal ethical and welfare committee of Nankai Hospital (NKYY-DWLL-2020-178), in accordance with the ARRIVE guideline.

2.5.2. Rat subcutaneous implant models. Ten male SD rats (8 week-old) were randomly divided into P34HB and P34HB/lec groups ($n = 5$). The rats were anesthetized with inhalation anesthesia (5% isoflurane). After dorsal hair shaving and sterilizing, an incision about 1 cm on the back of rat was made and the scaffold was implanted under the full thickness of the back flap. The rats were sacrificed at 4 weeks after surgery.

To assess the biocompatibility of the scaffolds *in vivo*, histological evaluation was applied. The scaffold with the soft tissue was fixed in 4% PFA for 1 day at room temperature and then dehydrated by a series of graded ethanol. The specimens were embedded, cut, and then stained with hematoxylin-eosin (HE). The prepared slices were observed by a microscope (Eclipse E100, Nikon).

2.5.3. Rat calvarial defect model. Twenty male SD rats (8 week-old) were randomly divided into P34HB and P34HB/lec groups ($n = 10$). All the rats were anesthetized and a longitudinal incision about 1.5 cm was made down to the periosteum. Then two full-thickness defects of 5 mm were created on both sides of the middle ridge with a trephine (1500 rpm).[43] The sterilized electrospun scaffolds were then implanted into the right calvarial defect area and the left calvarial defect was untreated as the blank group. Finally, the periosteum and skin of rats were closed carefully. The rats were sacrificed at 4 and 12 weeks after surgery.

Table 1 Primer sequences of target genes and GAPDH for real-time PCR assay

Target gene (rat)	Primer sequence (5′–3′)
ALP	F: CAACGTGGCCAAGAACATCA
	R: CCTGAGCGTTGGTGTTGTAC
Col1a1	F: GTACATCAGCCCAAACCCCA
	R: CAGGATCGGAACCTTCGCTT
GAPDH	F: AAACCCATCACCATCTTCCA
	R: GTGGTTCACACCCATCACAA

The calvariums with the scaffolds were fixed in 4% PFA for 3 days at room temperature and then scanned by a micro-CT scanner (Sky scan 1276, Bruker). After micro-CT scanning, the specimens were decalcified by the decalcification solution (Solarbio) for 3 weeks. The specimens were embedded, sectioned, and then HE staining as well as Masson's trichrome staining were conducted. The histological images were captured under a microscope (Eclipse E100, Nikon).

2.6. Statistical analysis

The results of this study were statistically analyzed with SPSS (v21.0, IBM) software. All quantitative data were shown as mean ± standard deviation (SD). Significant differences between groups were evaluated using one-way analysis of variance (ANOVA) and the statistical significance was accepted when $P < 0.05$.

3. Results

3.1. Characterization of P34HB/lecithin electrospun fiber scaffold

P34HB fiber scaffolds were prepared successfully through the electrospinning method. As illustrated in Fig. 1A and B, the continuous, round, uniform, and, nearly bead-free electrospun fibers were observed. These fibers were arranged randomly and interwoven with each other to form the porous scaffolds. In addition, Fig. 1B also presented that the surface of electrospun P34HB scaffold were coated with lecithin uniformly and the P34HB/lec scaffold still remained the porous structure.

To further illustrate the successful coating of lecithin, ATR-FTIR were performed (Fig. 1C). The FTIR spectrum of specimens in P34HB/lec groups showed a series absorbance peaks, including the peaks at 1782 cm^{-1} (C═O stretching), 1263 cm^{-1} (C–C–O stretching), 1115 cm^{-1} (C–O stretching), 1028 cm^{-1} (C–CO stretching), which were the same with the pure P34HB scaffolds (P34HB group).[44] In P34HB/lec groups, the P–O–C stretching at 1090 cm^{-1} and CH_2 functional groups at 2925 cm^{-1} (asymmetric), 2855 cm^{-1} (symmetric), and 721 cm^{-1} were observed, indicating the successful coating of lecithin on the scaffolds.

P34HB/lec scaffold showed a smaller water contact angle at 25.2 ± 4.4° than P34HB scaffold with 91.0 ± 1.7° contact angle ($P < 0.05$), indicating the improved hydrophilicity of P34HB/lec scaffold (Fig. 2A). P34HB and P34HB/lec nanofiber scaffolds as well as the saline group (negative control) showed the lower hemolysis than that of water group as the positive control, presenting an excellent hemocompatibility for P34HB nanofiber composite scaffolds with lecithin ($P < 0.05$) (Fig. 2B). Protein adsorption assay (Fig. 2C) revealed that no significant difference was observed between these two groups ($P > 0.05$).

3.2. *In vitro* cell study

3.2.1. Biocompatibility assay. BMSCs were observed under an optical microscopy (Primovert, Zeiss) and the cell surface

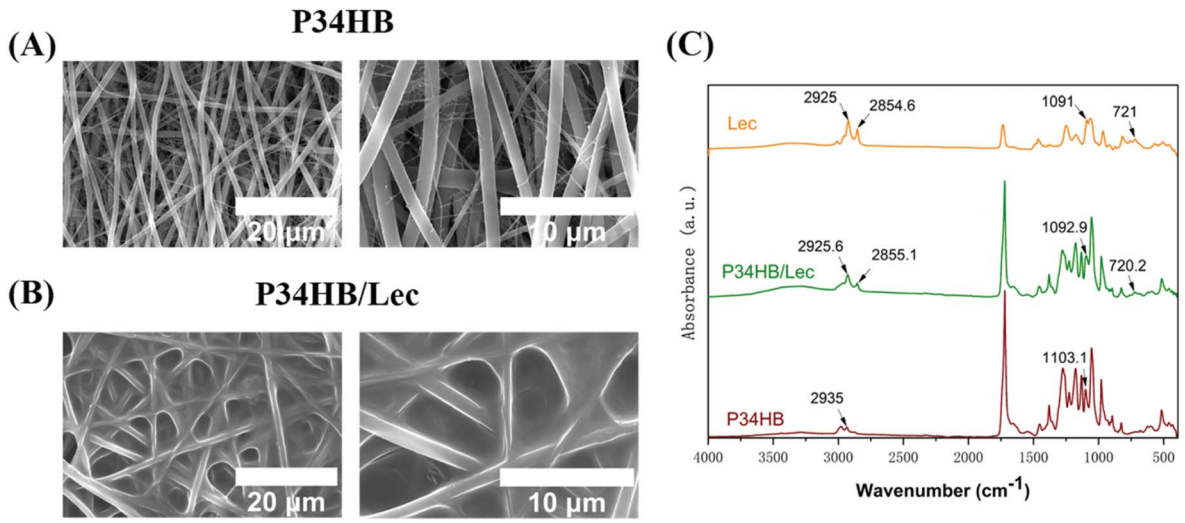

Fig. 1 (A) SEM images of P34HB scaffold; (B) SEM images of P34HB/lec scaffold; (C) FTIR spectra of P34HB, P34HB/lec, and lecithin.

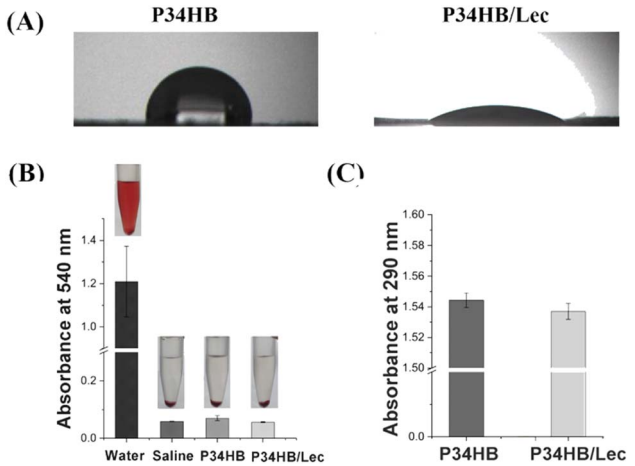

Fig. 2 (A) Water contact angles of P34HB scaffold and P34HB/lec scaffold; (B) hemolytic activity of P34HB scaffold and P34HB/lec scaffold; (C) protein adsorption P34HB scaffold and P34HB/lec scaffold.

markers detected by flow cytometry demonstrated that the obtained cells belonged to BMSCs (Fig. S1, details in ESI†).

As shown in Fig. 3A, CCK-8 assays revealed that BMSCs grew vigorously on the surface of these two groups after 3, 5, and 7 days. No significant difference was observed in the proliferation activity among all groups at 3 days ($P > 0.05$), while BMSCs in P34HB and P34HB/lec groups showed the higher proliferation than those in control group at 5 or 7 days ($P < 0.05$). Besides, there was no significant difference between P34HB and P34HB/lec groups at these time points ($P > 0.05$). According to Fig. 3B, after seeding on the scaffolds for 24 h, BMSCs were adhered tightly and stretched well on the fibers of scaffolds. Cells, exhibiting polygonal appearance on the crossed fibers, not only covered on the surface but also penetrated into the pores of P34HB scaffolds as well as P34HB/lec scaffolds.

As shown in Fig. 4, all the healing percentages of scratch area in P34HB/lec group at 8 h, 24 h, and 48 h were significantly higher than these in P34HB group, indicating a higher migration rate of BMSCs in P34HB/lec group. The results demonstrated that P34HB nanofibrous scaffolds with the lecithin could promote the migration of BMSCs.

3.2.2. Osteogenic differentiation. The results of ALP staining and quantitative ALP activity (Fig. 5A) showed that more ALP were secreted on P34HB/lec scaffold than P34HB scaffold on day 7 as well as day 14 ($P < 0.05$). The ECM mineralization of BMSCs was measured *via* Alizarin Red staining. Based on the optical images and the quantification result of ECM mineralization (Fig. 5B), no significant difference could be found between P34HB and P34HB/lec groups ($P > 0.05$). The expression levels of *ALP* and *Col1a1* mRNA after culturing for either 7 or 14 days were determined by RT-PCR. As shown in Fig. 5C, after culturing for 7 days, *ALP* gene expression in P34HB had no significant difference with that in P34HB/lec ($P > 0.05$), while there was much higher *Col1a1* expression in the cell cultured in P34HB/lec than in those on the P34HB scaffold ($P < 0.005$). Moreover, at day 14, the cells on P34HB/lec scaffold exhibited notably higher expression levels of *ALP* and *Col1a1* respectively, compared with the P34HB group ($P < 0.05$).

3.3. *In vivo* animal study

As shown in Fig. 6A, in the scaffolds implanted under the full thickness of the back flap, striated collagen bundles were distributed along the fibers and organization capsules were observed surrounding the specimens. The vascularization could also be found in these scaffolds, indicating the great biocompatibility of P34HB as well as P34HB/lec scaffolds.

As for the bone defect repair models, after 4 weeks and 12 weeks of surgery, the specimens were scanned and reconstructed by a micro-CT. 3D reconstructed images displayed that compared with the blank group, the other two groups presented greater new bone formations visually at 12 weeks after the surgery (Fig. 6B).

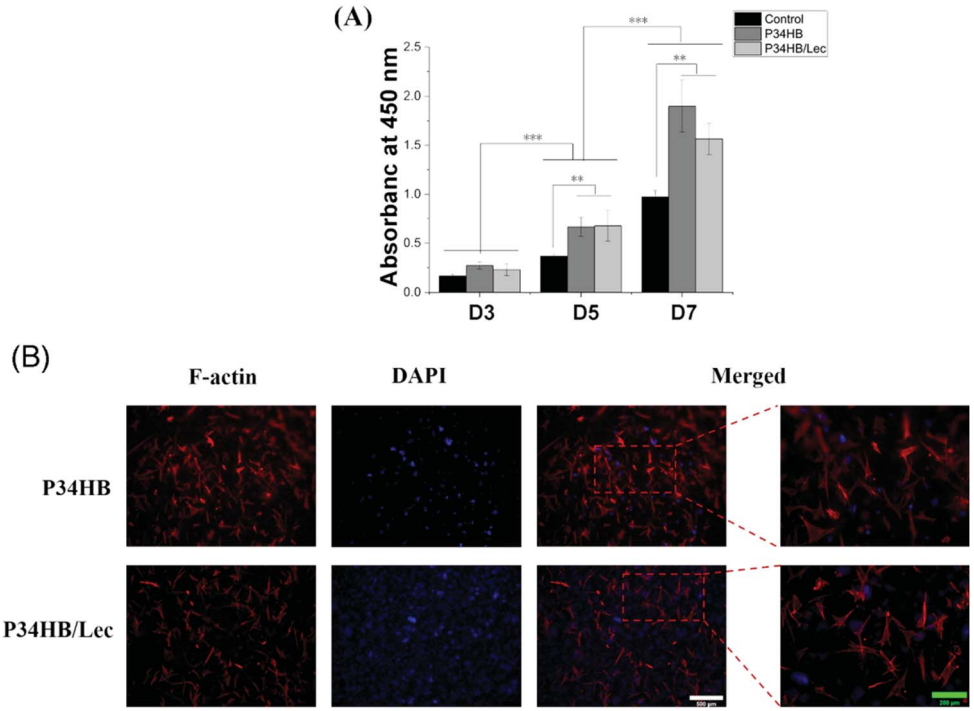

Fig. 3 (A) Cell proliferation examined *via* a CCK-8 assay after BMSCs were cultured for 3, 5, and 7 days; (B) confocal fluorescent microscopy of BMSCs cultured on P34HB and P34HB/lec scaffolds. White scale bar representing 500 μm; Green scale bar representing 200 μm; *P < 0.05, **P < 0.01, ***P < 0.005.

The results of P34HB scaffold and P34HB/lec groups showed more striated collagen bundles in the materials at 4 weeks and newly formed bone in the defect regions at 12 weeks, compared with the blank group. As shown in Fig. 6C and D, scattered collagen bundles came from the edge of the defects and stretched into the scaffolds, growing along the fibers. Moreover, denser collagen bundles as the bone-like tissues were observed near the defect edge in P34HB and P34HB/lec groups. The results of Masson's trichrome staining were consistent with those of HE staining and revealed that the scaffold facilitated bone tissue maturation as well.

4. Discussion

Bone defects, caused by trauma, tumors, infection, necrosis and so on, have posed a great challenge for clinical management. Since traditional clinical methods for bone repair have various deficiencies, bone tissue engineering has been introduced as a promising strategy with unique benefits.[45] The scaffold as a substitute for ECM was regarded as the essential key of bone tissue engineering, guiding the cell transplantation as well as the new bone growth.[5,32] It is necessary to establish an appropriate scaffold with excellent porous microstructure for bone defect and thereby promote the bone repair. In this study, the P34HB scaffold was prepared *via* a simple and efficient electrospinning technology, and then

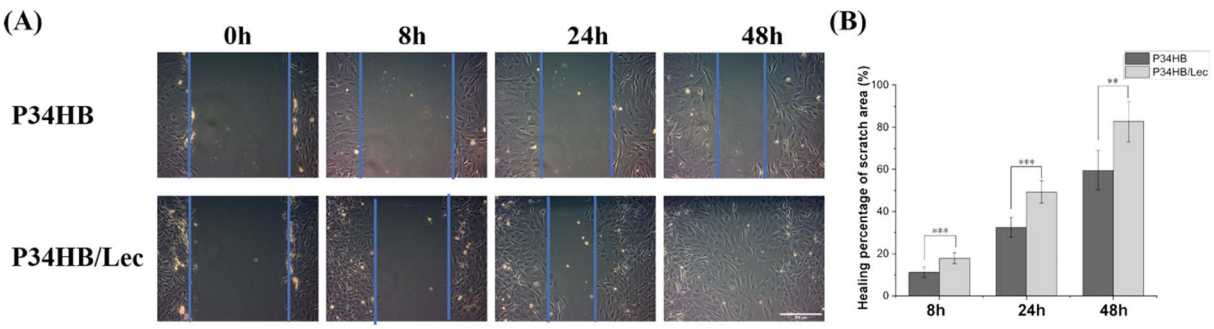

Fig. 4 (A) Scratch assay of cells in different groups culturing for 0, 8, 24, and 48 h under an optical microscope. (B) Healing percentages of scratch area in different groups. Scale bar representing 200 μm; *P < 0.05, **P < 0.01, ***P < 0.005.

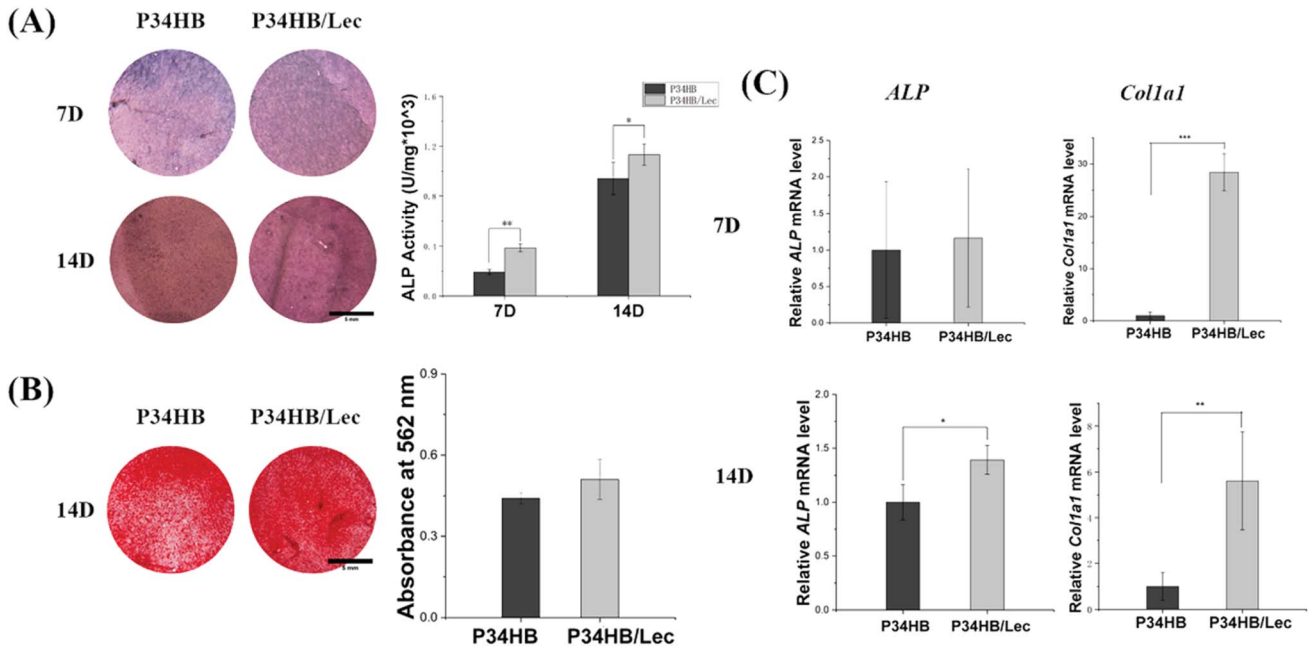

Fig. 5 (A) ALP staining and quantitative ALP activity of cells cultured on P34HB and P34HB/lec scaffolds at day 7 and day 14; (B) ECM mineralization and its colorimetric quantitative result of cells cultured on P34HB and P34HB/lec scaffolds at day 14; (C) expression of osteogenic-related genes in BMSCs cultured on different scaffolds measured by quantitative RT-PCR. Scale bar representing 1 mm; *P < 0.05, **P < 0.01, ***P < 0.005.

coated with lecithin. It was found that nanofibers of P34HB scaffolds in combination with the lecithin could exert a synergistic effect on promoting osteogenesis and regeneration of bone defects.

In this study, electrospun fibers were arranged randomly and interwoven with each other to form the porous scaffolds for the substitute of ECM in bone tissue engineering. As the electrospinning is a simple and versatile method to fabricate the polymer scaffolds, the electrospun fibers were obtained with an electrostatically driven jet of P34HB solution. As shown in the SEM images (Fig. 1), the fibers of P34HB scaffolds were arranged randomly and showed uniform diameter in nano scale. Besides, with the coated lecithin, P34HB/lec scaffold still remained the porous structure. According to CCK-8 results (Fig. 3A), BMSCs on P34HB and P34HB/lec scaffolds presented the higher proliferation than those in blank group, after cultured for 5 or 7 days. And the images of LSCM (Fig. 3B) also showed that BMSCs not only stretched well on the fibers of scaffolds at the early stage, but also penetrated into the pores of these scaffolds. The porous electrospun scaffolds offered a shelter for BMSCs and provided enough three-dimensional space for cell proliferation. Rough textured structures of P34HB scaffolds also supported the early adhesion of cells. Thus, the electrospun P34HB scaffolds simulated the formation of ECM, in which the oxygen and nutrients could transport to cells through the interconnected pores, and these scaffolds could exert enormous positive influence on the cellular adhesion, ingrowth, proliferation, and differentiation.[46,47]

In addition, lecithin coated on electrospun P34HB scaffolds could enhance the biocompatible and regenerative potential of these networks for bone tissue engineering. According to the results of water contact angles (Fig. 2A), P34HB/lec group showed a smaller contact angle than that of P34HB group. Thus, with the nature of being amphiphilic, soy lecithin created a hydrophilic surface of the scaffolds in P34HB/lec group. Due to poor hydrophilicity, the synthetic polymer scaffold showed little biological cues in ECM, and might even impede cell adhesion and penetration.[48,49] The addition of lecithin improved the hydrophilicity of pure P34HB scaffold, enhanced the efficiency of cell-seeding, and decreased inflammatory response, which could build an optimal microenvironment for bone tissue regeneration.[38] Furthermore, lecithin itself has a positive effect on physiological functions of cells with a stimulation of cell activity.[40] As the phospholipid from lecithin is an essential components of cell membranes, the migration of BMSCs were significantly promoted in P34HB/lec group compared with P34HB group (Fig. 4). Previous studies[37,39] have demonstrated that the incorporation of lecithin could promote cell growth, lead to milder immune response, and increase biocompatibility, which could play a positive role in promoting the osteogenic differentiation of BMSCs. As shown in Fig. 5C, compared to P34HB scaffold, P34HB/lec group showed higher expression level of *Col1a1* gene, presenting more secretion of type I collagen and osteogenic differentiation of BMSCs in P34HB/lec group. The high expression level of *Col1a1* gene might come from the addition of lecithin. On the one hand, lecithin could upregulate the expression levels of *Col1a1*, *OCN*, and *OPN* genes in MSCs directly.[50] On the other hand, by improving the hydrophilicity of scaffold, lecithin could influence the biological functions of cells such as cell attachment

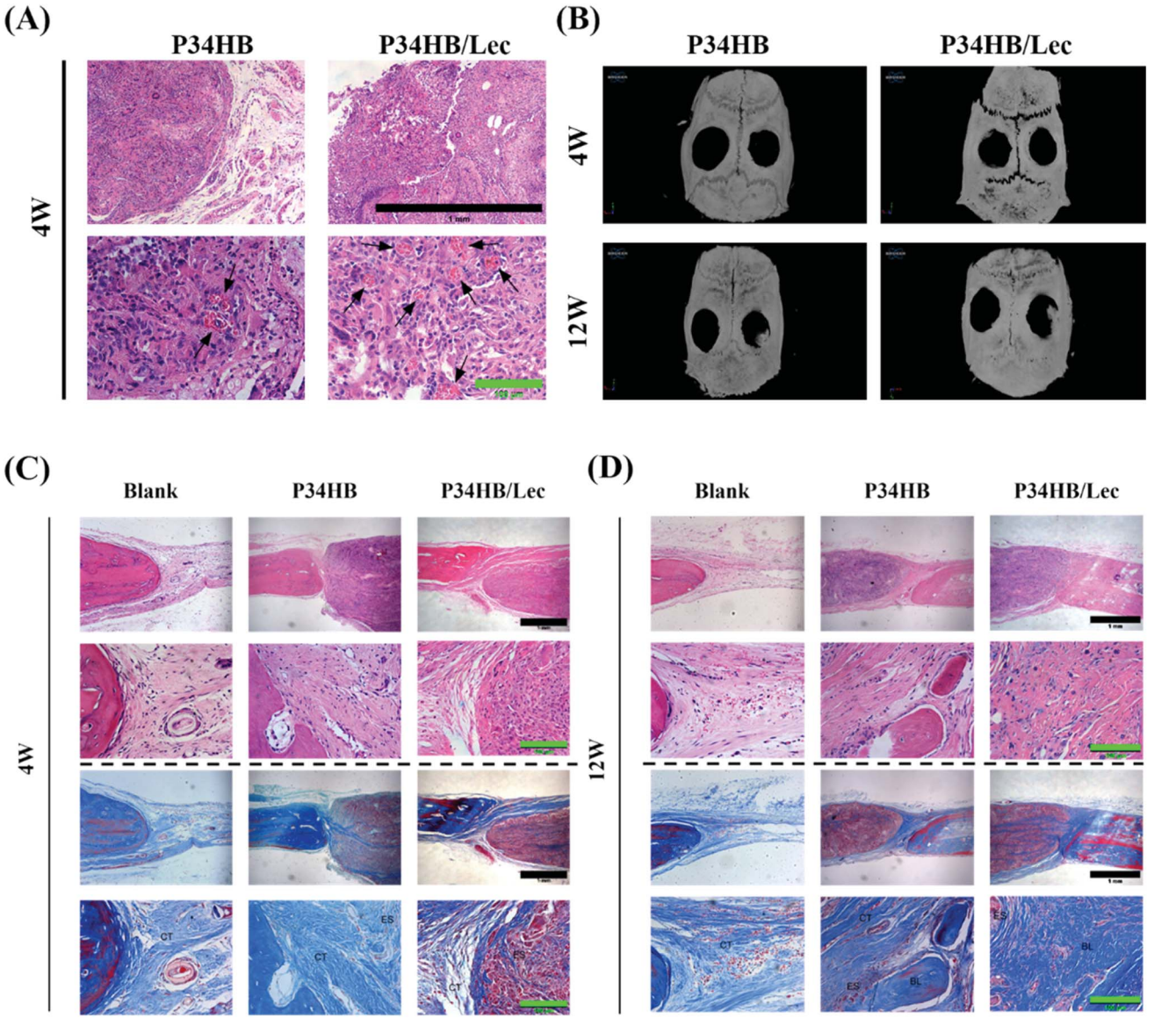

Fig. 6 (A) HE staining of the scaffolds implanted under the full thickness of the back flap after 4 weeks (black arrow: new vessel); (B) radiographical analysis of bone formation; (C) HE and Masson staining of repaired calvarial defects at 4 weeks (CT: connective tissue, ES: electrospun scaffold); (D) HE and Masson staining of repaired calvarial defects at 12 weeks (CT: connective tissue, ES: electrospun scaffold, BL: bone-like tissue). Black scale bar representing 1 mm; green scale bar representing 100 μm.

and migration,[35,51] which were also closely related to the expression of *Col1a1* gene. Hence, functionalization of electrospun P34HB scaffolds with lecithin can enhance the regenerative potential of these scaffolds for bone tissue engineering applications.

Both P34HB and lecithin represented excellent biocompatibility. No significant cytotoxicity of these scaffolds was observed to impact the proliferation and attachment of cells (Fig. 3). Furthermore, abundant striated collagen bundles and the vascularization was found in these scaffolds implanted under the back flap (Fig. 6A), presenting great biocompatibility of lecithin and P34HB. Accordingly, P34HB/lec scaffolds with good biocompatibility supported cellular attachment, remained cell bioactivity, and stimulated angiogenesis of tissue, which could be applied as bone tissue engineering scaffold for ECM.[38]

Hence, it was an efficient method to promote bone repair with porous electrospun P34HB/lec scaffold as the bone tissue engineering materials. The P34HB scaffold could be applied as the frame of ECM and lecithin could regulate biological functions of BMSCs. Based on the above results, electrospun P34HB/lec scaffold with preferable cellular affinity were supposed to be applied for bone tissue engineering. This current study still has some limitations and further investigations should be focused on improving the electrospun efficiency of P34HB scaffold and controlled-release of lecithin.

5. Conclusion

In this study, porous P34HB scaffolds with lecithin were successfully fabricated by electrospinning techniques for bone tissue regeneration. The scaffold provided porous space for cells and played enormous positive influence on the cellular biological functions. Though both P34HB and P34HB/lec scaffolds were capable of bone repair *in vivo*, P34HB/lec scaffold with lecithin coated on the surface presented great hydrophilicity and excellent biocompatibility. In addition, lecithin could promote cell migration and upregulated expression level of some osteogenesis genes. Therefore, P34HB scaffold with lecithin showed great application potential for bone tissue engineering.

Author contributions

Wei Liu: methodology, investigation, data curation, and writing – original draft preparation; Tiejun Jiao: methodology, investigation, and data curation; Yuran Su: investigation; Ran Wei: investigation; Zheng Wang: investigation; Jiacheng Liu: investigation; Lei Sui: supervision and writing – review & editing; Na Fu: conceptualization, methodology, supervision and writing – review & editing.

Conflicts of interest

There are no conflicts of interest to declare.

Acknowledgements

This work was financially supported by the National Natural Science Foundation of China (No. 81800930, No. 81970958). The funders had no role in study design, data collection and analysis, decision to publish, or preparation of the manuscript.

References

1 V. S. Waghmare, P. R. Wadke, S. Dyawanapelly, A. Deshpande, R. Jain and P. Dandekar, *Bioact. Mater.*, 2018, **3**, 255–266.
2 N. Fu, S. Deng, Y. Fu, G. Li, X. Cun, L. Hao, X. Wei, X. Cai, Q. Peng and Y. Lin, *Cell Proliferation*, 2014, **47**, 465–475.
3 D. Zhao, L. Lei, S. Wang and H. Nie, *J. Mater. Chem. B*, 2015, **3**, 7319–7333.
4 L. R. Lizarraga-Valderrama, C. S. Taylor, F. Claeyssens, J. W. Haycock, J. C. Knowles and I. Roy, *J. Tissue Eng. Regener. Med.*, 2019, **13**, 1581–1594.
5 M. X. Ma, Q. Liu, C. Ye, B. Grottkau, B. Guo and Y. F. Song, *BioMed Res. Int.*, 2017, **2017**, 9251806.
6 Y. He, Y. Zhong, Y. Su, Y. Lu, Z. Jiang, F. Peng, T. Xu, S. Su, Q. Huang, C. Fan and S. T. Lee, *Angew. Chem., Int. Ed. Engl.*, 2011, **50**, 5695–5698.
7 R. Schlapak, J. Danzberger, D. Armitage, D. Morgan, A. Ebner, P. Hinterdorfer, P. Pollheimer, H. J. Gruber, F. Schäffler and S. Howorka, *Small*, 2012, **8**, 89–97.
8 Y. Zhao, J. Zhou, Z. Jia, D. Huo, Q. Liu, D. Zhong, Y. Hu, M. Yang, M. Bian and C. Hou, *Mikrochim. Acta*, 2019, **186**, 92.
9 A. Rodriguez-Contreras, *Bioengineering*, 2019, **6**, 82–95.
10 Y. Li, C. Han, Y. Yu and D. Huang, *Int. J. Biol. Macromol.*, 2019, **129**, 1–12.
11 C. Zhijiang, Z. Qin, S. Xianyou and L. Yuanpei, *Mater. Sci. Eng., C*, 2017, **71**, 797–806.
12 C. L. Dong, S. Y. Li, Y. Wang, Y. Dong, J. Z. Tang, J. C. Chen and G. Q. Chen, *Biomaterials*, 2012, **33**, 2593–2599.
13 R. Luo, K. Xu and G.-Q. Chen, *J. Appl. Polym. Sci.*, 2007, **105**, 3402–3408.
14 J. Zhang, E. I. Shishatskaya, T. G. Volova, L. F. da Silva and G. Q. Chen, *Mater. Sci. Eng., C*, 2018, **86**, 144–150.
15 Y. Y. Shangguan, Y. W. Wang, Q. Wu and G. Q. Chen, *Biomaterials*, 2006, **27**, 2349–2357.
16 G. J. M. de Koning, M. Kellerhals, C. van Meurs and B. Witholt, *Bioprocess Eng.*, 1997, **17**, 15–21.
17 P. K. Samantaray, A. Little, A. M. Wemyss, E. Iacovidou and C. Wan, *ACS Sustainable Chem. Eng.*, 2021, **9**, 9151–9164.
18 J. Sun, Z. Dai, Y. Zhao and G. Q. Chen, *Biomaterials*, 2007, **28**, 3896–3903.
19 P. K. Samantaray, A. Little, D. M. Haddleton, T. McNally, B. Tan, Z. Sun, W. Huang, Y. Ji and C. Wan, *Green Chem.*, 2020, **22**, 4055–4081.
20 T. Volova, E. Shishatskaya, E. Nikolaeva and A. Sinskey, *Mater. Sci. Technol.*, 2014, **30**, 549–557.
21 M. Koller, *Molecules*, 2018, **23**, 362–381.
22 Y.-X. Ma, J.-S. Mu, J.-Q. Zhang and P. Bo, *J. Biomater. Tissue Eng.*, 2016, **6**, 629–634.
23 Z. Su, P. Li, B. Wu, H. Ma, Y. Wang, G. Liu, H. Zeng, Z. Li and X. Wei, *Mater. Sci. Eng., C*, 2014, **45**, 374–382.
24 E. I. Shishatskaya, E. D. Nikolaeva, O. N. Vinogradova and T. G. Volova, *J. Mater. Sci.: Mater. Med.*, 2016, **27**, 165.
25 D. H. Reneker and A. L. Yarin, *Polymer*, 2008, **49**, 2387–2425.
26 G. H. Kim, *Biomed. Mater.*, 2008, **3**, 025010.
27 J. Xue, J. Xie, W. Liu and Y. Xia, *Acc. Chem. Res.*, 2017, **50**, 1976–1987.
28 Z. Zhu, Y. Liu, Y. Xue, X. Cheng, W. Zhao, J. Wang, R. He, Q. Wan and X. Pei, *ACS Appl. Mater. Interfaces*, 2019, **11**, 36141–36153.
29 N. Fu, J. Xie, G. Li, X. Shao, S. Shi, S. Lin, S. Deng, K. Sun and Y. Lin, *RSC Adv.*, 2015, **5**, 21572–21579.
30 Z. Wang, K. Ma, X. Jiang, J. Xie, P. Cai, F. Li, R. Liang, J. Zhao and L. Zheng, *Mater. Sci. Eng., C*, 2020, **112**, 110763.
31 T. Zhou, G. Li, S. Lin, T. Tian, Q. Ma, Q. Zhang, S. Shi, C. Xue, W. Ma, X. Cai and Y. Lin, *ACS Appl. Mater. Interfaces*, 2017, **9**, 42589–42600.
32 T. Zhou, G. Li, S. Lin, S. Shi, J. Liao, T. Tian, Q. Huang and Y. Lin, *J. Biomed. Nanotechnol.*, 2017, **13**, 822–834.
33 A. Tang, J. Li, S. Zhao, T. Liu, Q. Wang and J.-F. Wang, *J. Nanosci. Nanotechnol.*, 2017, **17**, 3888–3895.
34 S. Mathews, K. Kaladhar and C. P. Sharma, *J. Biomed. Mater. Res., Part A*, 2006, **79**, 147–152.
35 X. Shi, Y. Wang, L. Ren, W. Huang and D. A. Wang, *Int. J. Pharm.*, 2009, **373**, 85–92.
36 N. Zhu, F. Z. Cui, K. Hu and L. Zhu, *J. Biomed. Mater. Res., Part A*, 2007, **82**, 455–461.

37 Y. Wang, F. Z. Cui, Y. P. Jiao, K. Hu and D. D. Fan, *Biomed. Mater.*, 2008, **3**, 015012.
38 T. Matson, J. Gootee, C. Snider, J. Brockman, D. Grant and S. A. Grant, *J. Biomater. Appl.*, 2019, **33**, 979–988.
39 M. Zhang, K. Wang, Z. Wang, B. Xing, Q. Zhao and D. Kong, *J. Mater. Sci.: Mater. Med.*, 2012, **23**, 2639–2648.
40 E. Arab Tehrany, C. J. Kahn, C. Baravian, B. Maherani, N. Belhaj, X. Wang and M. Linder, *Colloids Surf., B*, 2012, **95**, 75–81.
41 W. Shao, J. He, Q. Wang, S. Cui and B. Ding, *ACS Biomater. Sci. Eng.*, 2017, **3**, 1370–1380.
42 X. Li, Y. Zhang and G. Qi, *Cytotechnology*, 2013, **65**, 323–334.
43 P. P. Spicer, J. D. Kretlow, S. Young, J. A. Jansen, F. K. Kasper and A. G. Mikos, *Nat. Protoc.*, 2012, **7**, 1918–1929.
44 J. Pan, G. Li, Z. Chen, X. Chen, W. Zhu and K. Xu, *Biomaterials*, 2009, **30**, 2975–2984.
45 N. Fu, Z. Meng, T. Jiao, X. Luo, Z. Tang, B. Zhu, L. Sui and X. Cai, *Cell Proliferation*, 2019, **52**, e12601.
46 R. Ravichandran, C. Ng, S. Liao, D. Pliszka, M. Raghunath, S. Ramakrishna and C. K. Chan, *Biomed. Mater.*, 2012, **7**, 015001.
47 M. Kharaziha, M. H. Fathi and H. Edris, *J. Mech. Behav. Biomed. Mater.*, 2013, **24**, 9–20.
48 J. Wang, D. Li, T. Li, J. Ding, J. Liu, B. Li and X. Chen, *Materials*, 2015, **8**, 1009–1026.
49 Y. C. Shin, J. H. Lee, L. Jin, M. J. Kim, C. Kim, S. W. Hong, J. W. Oh and D. W. Han, *J. Nanosci. Nanotechnol.*, 2015, **15**, 7907–7912.
50 B. D. M. Coverdale, J. E. Gough, W. W. Sampson and J. A. Hoyland, *J. Biomed. Mater. Res., Part A*, 2017, **105**, 2865–2874.
51 X. Shi, Y. Wang, L. Ren, C. Lai, Y. Gong and D. A. Wang, *J. Biomed. Mater. Res., Part A*, 2010, **92**, 963–972.